

The Twelfth East Asia-Pacific Conference on Structural Engineering and Construction

## Microstructure Analysis of Heated Portland Cement Paste

Qi Zhang and Guang Ye

*Microlab, Delft University of Technology, 2628 CN Delft, the Netherlands*

---

### Abstract

When a concrete structure is exposed to high temperature, the mechanical damage and chemical transformation take place simultaneously, which will change the microstructure of material. On the other hand, the mechanical properties and transport properties depend on the development of microstructure of cement paste. In order to study the microstructure changes at high temperature, in this contribution the cement paste samples were firstly heated to varied temperatures from 100 °C to 1000 °C with heating rate of 5°C/min, and then naturally cooled to indoor temperature. In the microstructural analysis program, the environmental scanning electron microscope (ESEM), mercury intrusion porosimetry (MIP) and thermogravimetry analysis (TGA) were used. The images captured by ESEM were analyzed by segmentation and binary image processing in order to calculate the volume fractions of hydration products and porosity. The change on density distribution of hydration products was characterized by histogram of ESEM image at different temperatures. The porosity and pore size distribution of same samples were studied by MIP and the chemical decomposition was analyzed by TGA as well. Through the analysis of the information obtained from TGA and microstructure measurements, it is found that hydrated calcium silicate (CSH gel) and portlandite dehydrated into sparse crystalline particles when temperature reached 1000 °C. The porosity and the connectivity of pore of cement paste increased along with temperature increase. The results of this research provide a fundamental understanding on how the fire sapling occurs when concrete structures were exposed to high temperature.

© 2011 Published by Elsevier Ltd. Selection and/or peer-review under responsibility of [name organizer]

*Keywords:* Microstructure, cement paste, high temperature, ESEM, MIP.

---

## 1. INTRODUCTION

The performances of cement paste are governed by its microstructure, in particular the pore network plays a critical role in determining the transport properties and mechanical properties. When a concrete structure is exposed to high temperatures, the microstructures of cement paste change due to the complex physical-chemical reaction. To better understand the behavior of fire spalling, investigation of microstructure of cement paste exposed to high temperature is necessary.

Lots of investigations of cement pastes by backscatter electron microscopy (BSEM) have been carried out in past decades (Lange, Sujata et al. 1991; Lange, Jennings et al. 1994; Scrivener 2004; Diamond and Kjellsen 2006). The SEM image demonstrates not only the pore structure but also the phase morphology. Several methods have reported to characterize the SEM image, including stereological analysis (Nemati and Stroeven 2001) and phase separating (Scrivener 2004). Torquato (Torquato 2001) summarized the relation functions to characterize the porous material, and Bentz et al. (Bentz, Stutzman et al. 1999) employed the relationship functions to describe the SEM image of cement paste.

Mercury intrusion porosimetry (MIP) is another useful technique to measure pore size distribution of cement paste (Diamond 1971; Cook and Hover 1991; Cook and Hover 1993; Cook and Hover 1999; Diamond 2000; Diamond and Kjellsen 2006). The pore diameters that can be measured by MIP vary from 0.001  $\mu\text{m}$  to 1000  $\mu\text{m}$  according to the pressure used.

In this contribution, the microstructure of heated cement paste was investigated by both environmental scanning electron microscope (ESEM) and Mercury intrusion porosimetry (MIP). In conjunction with a backscatter electron (BSE) detector, the densities of different phases are represented in the images by gray level variation. The phases in SEM images were separated by graphic techniques to extract the features of microstructure. By combining the SEM image and MIP results, a more complete picture of pore structure is presented. The weight loss of cement paste during heating was measured by thermogravimetry (TG). The relationship of weight loss due to dehydration and microstructure development was discussed finally.

## 2 EXPERIMENT METHOD

All experiment were carried out using an ordinary Portland cement (OPC), CEM I 42.5N. The cement paste was prepared with water/cement ratio 0.50. The cement paste was cast in small closed plastic bottles. After being cured for 28 days, the hardened paste cylinders were removed from the plastic bottles and cut into small pieces (<5g) for ESEM and MIP. Before measurement, the cement paste pieces were stored in the furnace at various constant temperatures from 105°C to 1000°C for 24 hours.

The samples for ESEM were impregnated with an epoxy resin under low vacuum, and polished with silicon carbide grit from 6  $\mu\text{m}$  to 0.25  $\mu\text{m}$ . Twenty digital images of each cut surface were captured by using a backscattering detector at a magnification of 500 and 2000 with a voltage of 17 KV.

For thermal analysis, the cement paste samples were grinded into small powders (<50  $\mu\text{m}$ ). The simultaneous thermogravimetry analyzer was used to measure the TG and DSC. The instrument allows the measurement of mass changes and thermal effects between -150°C and 1500°C. The purge gas was nitrogen, and the gas velocity was 20ml/min. The sample was heated with rate of 10°C/min from 30°C to 1000°C.

## 3. EXPERIMENT RESULTS

### 3.1 Scanning Electron Microscopy

### 3.1.1 Morphological characterization

The BSE micrographs of cement paste samples heated at different temperature were shown in Figure 1. The gray levels of digital images reflect the density difference of phases in cement paste. The typical histograms of gray level of heated cement paste were selected and shown in Figure 2. By visual observation of digital images and its histogram, the microstructural development process can be divided into three steps:

- From 30°C to 400°C, the microstructure of cement paste didn't change too much. The CSH kept gel-like morphology. The profiles of gray-level histograms from 103°C to 400°C were similar (see Figure 2). Four peaks could be found in these histograms, which represent capillary pore, low density hydrates, high density hydrates and clinker, respectively. The high density hydrates include high density calcium silicate hydrate (CSH) and calcium hydroxide (CH), and low density hydrates mainly refer low density calcium silicate hydrate (CSH).
- From 500°C to 800°C, due to the volume change of hydrate, cracks occur in the cement paste matrix. The isolated pores in the cement paste matrix became connected with each others. The two peaks represented hydrates (CSH and CH) in the histogram merged into one peak, which means both high density hydrates and low density hydrates transferred into the dehydration products with similar density. By the comparing the grey level of CSH with clinker's, the gel-like CSH shrunk gradually and became more and more dense.
- At about 1000°C, the hydrates including CSH and CH were transferred into crystalline-like phase completely. The pore system seriously expanded. Three peaks in histogram can be found. The two peaks represented hydrates and clinkers were very low.

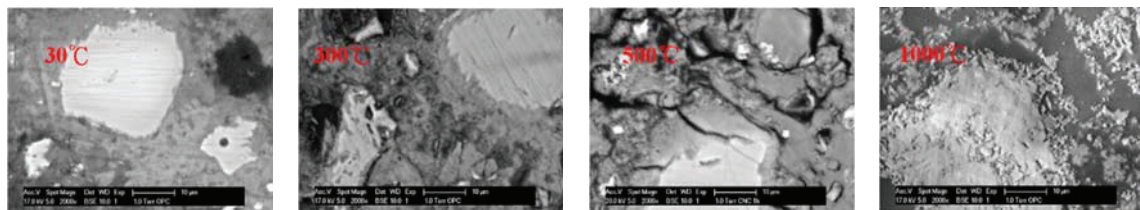


Figure 1: BSE images of heated cement paste at different temperatures.

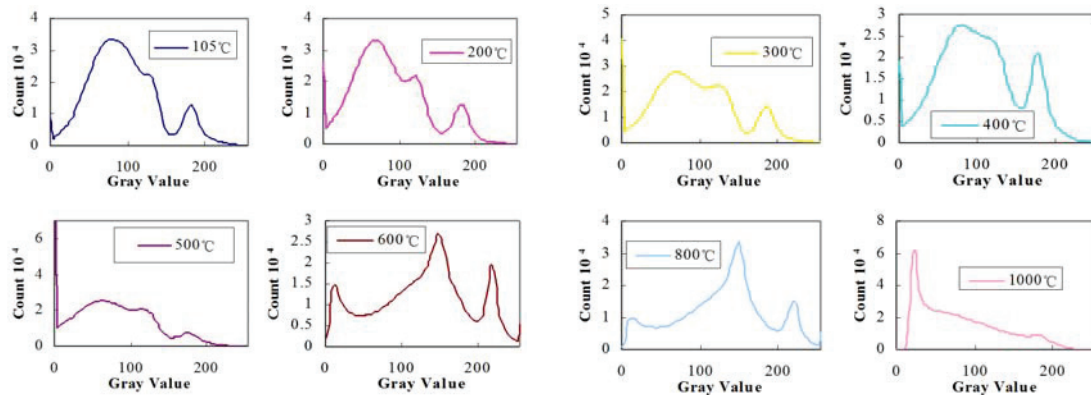


Figure 2: Gray levels histogram of BSE images of heated cement paste at different temperatures.

### 3.1.2 Image analysis

The BSE images were analyzed by using thresholding techniques. From grey levels histogram, the threshold of each phase was distinguished by finding the valleys in the histogram curve. The area fraction of each phase on image was calculated. Detailed description of this technique is referred to (Silva, de Alencar Lotufo et al. 2002). In this study, 15 images with magnification of 500 for each sample were acquired and analyzed. According to the peak number in histogram, the cement paste was divided into four phases when the samples were heated from 30°C to 500°C, and was divided into three phases when the samples were heated from 600°C to 1000°C. The results of image analysis, including both the average area fraction and the coefficient of standard deviation, were listed in Table 1. It can be found that the pore area fraction increased slowly before 400°C, and increased rapidly after 400°C. This may be due to the decomposition of CH between 400°C to 500°C. The hydrate phase area fraction decreased continuously.

Table 1: Phase area percentage: mean value and standard deviation from digital image analysis

Temperature (°C)	Pore (%)		Low density hydrates (%)		High density hydrates (%)		Dehydration product (%)		Clinker (%)	
	x	ε	x	ε	x	ε	x	ε	x	ε
30	9.42	5.03	65.39	6.76	14.50	4.17	-----	-----	10.69	0.51
105	9.08	2.68	65.27	3.62	15.45	3.74	-----	-----	10.19	1.15
200	9.99	3.71	58.86	6.74	20.56	3.59	-----	-----	10.59	2.57
300	8.79	1.79	55.22	3.43	24.57	2.85	-----	-----	11.42	3.09
400	11.22	4.85	48.46	7.85	26.68	2.34	-----	-----	13.64	3.62
500	16.62	2.66	43.52	4.34	26.65	2.69	-----	-----	13.22	4.41
600	18.66	3.22	-----	-----	-----	-----	68.10	3.44	13.24	4.32
800	20.76	2.43	-----	-----	-----	-----	66.70	4.54	12.54	5.93
1000	24.69	1.66	-----	-----	-----	-----	61.78	4.77	13.53	3.13

### 3.2 Mercury intrusion porosimetry

The mercury intrusion curves provide the total porosity. The intrusion curves of samples were shown in Figure 3(a). The total pore volume of samples increased along with temperature increase. The volumes of capillary pore ( $>1\mu\text{m}$ ) of samples from  $105^\circ\text{C}$  to  $400^\circ\text{C}$  were very close. When temperature change from  $400^\circ\text{C}$  to  $500^\circ\text{C}$ , it is evident that both capillary pore ( $>0.01\mu\text{m}$ ) and gel pore ( $<0.01\mu\text{m}$ ) increased seriously. This may be due to the decomposition of CH between  $400^\circ\text{C}$  to  $500^\circ\text{C}$ . The pore size distribution differential curve is obtained by taking the slope of the pore size distribution curve the Log Differential Intrusion against pore sizes Figure 3(b). For cement paste, several peaks can be found from this curve. These peaks represent the pore diameters corresponding to the higher rate of mercury intrusion per change in pressure. These peaks are called “threshold” pore diameters. The threshold pore diameters of samples could be observed from the Log Differential Intrusion versus pore size curves in Figure 3(b). Two peaks could be found in the curve of sample heated at  $105^\circ\text{C}$ . But only one peak could be found in other temperatures in Figure 3(b). This may be caused by the enlargement of gel pore due to dehydration.

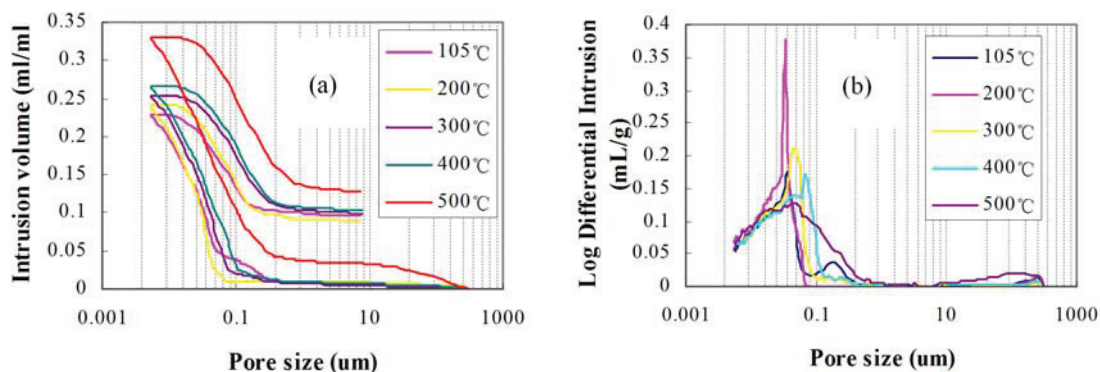


Figure 3: MIP results of cement paste samples after exposure to heating

### 3.3 Thermal analysis

The results of thermogravimetry analysis obtained at a heating rate of  $10^\circ\text{C}/\text{min}$  were summarized in Figure 4(a). Weight lost rapidly at the beginning of heating, and then the rate of weight loss became lower and lower. It can be observed that the weight lost rapidly at about  $450^\circ\text{C}$ , which was caused by the dehydration of calcium hydroxide. By comparison of the porosity against temperature curves measured by MIP and ESEM separately in Figure 4(a), it can be found that the trends of porosity development of these two curves were similar. The porosity tested by MIP was larger than the results by ESEM. This was due to the measurement theory difference of two methods. Because of the limitation of resolution, ESEM images can't measure the pore size smaller than resolution of image. MIP can detect both capillary pore and gel pore only if they are connected. By combining the porosity curves with weight loss curve, it can be observed that the capillary pores didn't change too much before  $400^\circ\text{C}$  when the weight lost rapidly. However, when the weight lost slowly after  $500^\circ\text{C}$ , the capillary pores expanded obviously.

The dehydration degree was defined as the ratio of weight loss due to dehydration and maximum water content. The hydrates area fraction in ESEM image against the dehydration degree was plotted in Figure 4(b) in order to reveal the relationship between the volume change of hydrates and dehydration. This curve can be divided into three stages according to the slopes:

- Before the dehydration degree 0.3, the hydrates volume changed very little. This means that the dehydration didn't break the CSH gel-like framework.
- When the dehydration degree was between 0.3 and 0.9, the hydrates volume changed in proportion to the dehydration degree.
- After the dehydration degree 0.9, the hydrates shrank rapidly.

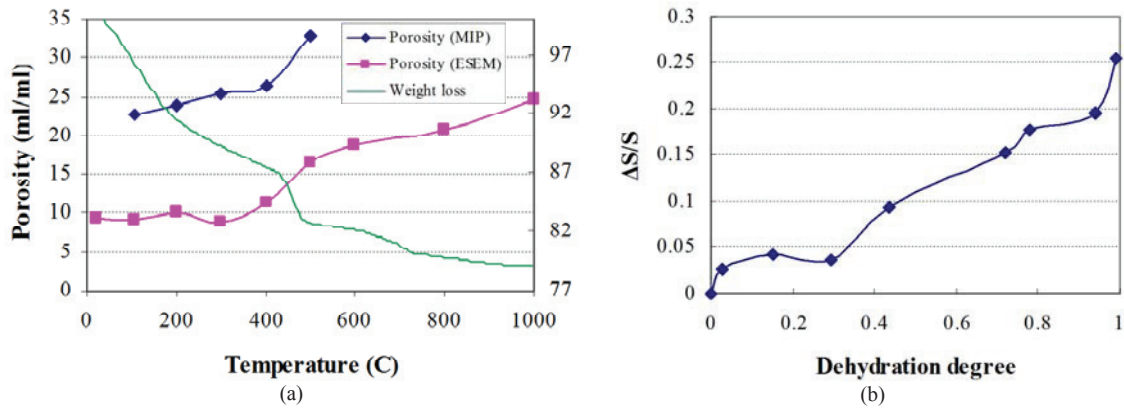


Figure 4: (a) The weight loss curve and porosity development versus temperature; (b) The hydrate area fraction in ESEM image against dehydration degree.

#### 4. CONCLUSIONS

In this paper, the cement paste samples fired to various temperatures from 105°C to 1000°C have been studied by ESEM and MIP. The microstructural investigation demonstrated that the morphology of cement paste changed continuously along with the increasing of temperature. By combining the microstructural measurement results with thermal analysis results, the conclusions of this study were summarized below:

- The BSE images have shown that the gel-like CSH start to shrink rapid at 500°C, and became into crystalline phase partly at 1000°C. The image analysis by thresholding technique revealed the development of phase distribution during heating. At high temperature, the hydrates in cement paste shrunk and became more and more dense.
- The porosities of the samples determined by MIP were larger than that determined by BSE image analysis. But the trends of development porosity determined by both techniques shown good agreement with each other.
- By comparing the porosity determined by MIP and BSE image analysis with the weight loss determined by TGA, the relationship of the capillary pore and the dehydration was studied. The capillary pore didn't change significant before 400°C, but the weight lost rapidly. When the weight lost slowly after 400°C, the capillary pore expanded seriously.
- The empirical relationship between the changes of the volume of hydrates and degree of dehydration was presented.

#### References

- [1] Bentz, D. P., P. E. Stutzman, et al. (1999). SEM/X-RAY IMAGING OF CEMENT-BASED MATERIALS. Microscopy Applied to Building Materials, 7th Euroseminar. Proceedings, Delft, The Netherlands.



- [2] Cook, R. A. and K. C. Hover (1991). "Experiments on the contact angle between mercury and hardened cement paste." *Cement and Concrete Research* **21**(6): 1165-1175.
- [3] Cook, R. A. and K. C. Hover (1993). "Mercury porosimetry of cement-based materials and associated correction factors." *Construction and Building Materials* **7**(4): 231-240.
- [4] Cook, R. A. and K. C. Hover (1999). "Mercury porosimetry of hardened cement pastes." *Cement and Concrete Research* **29**(6): 933-943.
- [5] Diamond, S. (1971). "A critical comparison of mercury porosimetry and capillary condensation pore size distributions of portland cement pastes." *Cement and Concrete Research* **1**(5): 531-545.
- [6] Diamond, S. (2000). "Mercury porosimetry: An inappropriate method for the measurement of pore size distributions in cement-based materials." *Cement and Concrete Research* **30**(10): 1517-1525.
- [7] Diamond, S. and K. O. Kjellsen (2006). "Resolution of fine fibrous C-S-H in backscatter SEM examination." *Cement and Concrete Composites* **28**(2): 130-132.
- [8] Lange, D. A., H. M. Jennings, et al. (1994). "Image analysis techniques for characterization of pore structure of cement-based materials." *Cement and Concrete Research* **24**(5): 841-853.
- [9] Lange, D. A., K. Sujata, et al. (1991). "Observations of wet cement using electron microscopy." *Ultramicroscopy* **37**(1-4): 234-238.
- [10] Nemati, K. and P. Stroeve (2001). "Stereological analysis of micromechanical behavior of concrete." *Materials and Structures* **34**(8): 486-494.
- [11] Scrivener, K. L. (2004). "Backscattered electron imaging of cementitious microstructures: understanding and quantification." *Cement and Concrete Composites* **26**(8): 935-945.
- [12] Silva, A. G., R. de Alencar Lotufo, et al. (2002). Classification of microstructures by morphological analysis and estimation of the hydration degree of cement paste in concrete. *Computer Graphics and Image Processing, 2002. Proceedings. XV Brazilian Symposium on*.
- [13] Torquato, S. (2001). *Random Heterogeneous Materials*, Springer.